IEEE Access
Multidisciplinary | Rapid Review | Open Access Journal

Received April 29, 2019, accepted May 18, 2019, date of publication May 22, 2019, date of current version June 5, 2019.

*Digital Object Identifier 10.1109/ACCESS.2019.2918344*

# Experimental Evaluation of the Tri-Polarized MIMO Channel Properties Based on a Compact Multimode Antenna

**DAZHI PIAO AND YAJIN WANG**
Department of Communication Engineering, Communication University of China, Beijing 100024, China
Key Laboratory of Media Audio and Video of Ministry of Education, Communication University of China, Beijing 100024, China

Corresponding author: Dazhi Piao (piaodazhi@cuc.edu.cn)

This work was supported by the National Natural Science Foundations of China under Grant 61771435.

**ABSTRACT** Based on a planar and compact antenna, extensive measurements are conducted to investigate the behavior of the colocated tri-polarized multiple-input multiple-output (MIMO) system working at 3.5 GHz. Several scenarios with different multipath distributions have been considered, including a reverberation chamber (RC) and also some line-of-sight (LOS) and obstructed LOS (OLOS) real-world indoor environments. Many channel parameters of the MIMO system are analyzed based on the measured data, including cross-polarization discrimination (XPD), Ricean $K$-factor, correlation coefficient (CC), MIMO channel capacity gain (CG), channel eigenvalues, and ellipticity statistic (ES). The results show that for a multi-polarized MIMO system, the effects of polarization coupling and transition depend strongly on the polarimetric scattering characteristic of the environments. Furthermore, in all the scenarios tested, three non-zero eigenvalues of the MIMO channel matrix are obtained, which indicates that three independent subchannels can be supported by the tri-polarized MIMO system.

**INDEX TERMS** Tri-polarized antenna, multiple-input multiple-output (MIMO), cross-polarization discrimination (XPD), Ricean $K$-factor, MIMO channel capacity gain (CG), measurement.

## I. INTRODUCTION

The tri-polarized antenna has a potential to provide one more degree of freedom over the dual-polarized one, since multiple components of the electromagnetic field can be sensed [1]–[5]. Thus, the compact and colocated tri-polarized antenna could be a good candidate for the dense massive multiple-input multiple-output (MIMO) array. Many designs of colocated tri-polarized antenna have been realized by different combinations of dipole, loop, monopole, slot and patch antennas [6]–[18]; however, those antennas are rarely realized by a compact and planar structure, moreover, few studies about the tri-polarized MIMO channel performance in relation to the actual propagation conditions have been conducted.

In the controlled rich scattered laboratory environment, some tri-polarized MIMO propagation measurements have been performed. Three parallel spatial channels and nearly three-fold increase in channel capacity by the tri-polarized antenna with respect to the uni-polarized one has been demonstrated, using tri-polarized antenna containing one loop and two dipoles at 2.25 GHz [4], 3 dipoles at 3.85 GHz [6], 3 dipoles and 3 slots at 2.55 GHz [7], and a dual-polarized patch and a monopole at 2.2 GHz [11]. The MIMO performances were also compared between a tri-polarized loop and a tri-polarized dipole at 2.45 GHz [8] in the reverberation chamber (RC) and some indoor environments.

In this paper, extensive channel measurements have been conducted at 3.5 GHz based on our designed tri-polarized antenna [19], which is an important sub 6 GHz frequency band in the fifth-generation mobile communication (5G) system [20], [21]. This colocated tri-polarized antenna is realized by a very compact single-layer patch structure, using the mode $TM_{02}$ producing a vertical monopole-like radiation pattern, and two orthogonally exited $TM_{11}$ modes with microstrip-like patterns. Furthermore, this tri-polarized antenna has a planar structure, with a total height of 3.0 mm and radius of 25 mm.

To investigate the effects of the distribution and richness of multipath on the polarization coupling effect and the multiplexing capability of the tri-polarized MIMO system, many scenarios with different multipath distributions have

The associate editor coordinating the review of this manuscript and approving it for publication was Chan Hwang See.

been considered, including the rich scattered RC and also some line-of-sight (LOS) indoor environments. Furthermore, an obstructed LOS (OLOS) case is also investigated, in which the transmitting (Tx) and receiving (Rx) antennas are separated by a rectangular pillar. The MIMO performances in this case are obviously different from that in the other scenarios having a strong LOS signal, caused by the rich diffuse scattering produced by the edges of the pillar. During the measurement, different heights and orientations of the antennas with varying communication distance are investigated. Furthermore, comprehensive analyses have been made about the channel parameters based on the measured data, including cross-polarization discrimination (XPD), Ricean K-factor, correlation coefficient (CC), and channel ellipticity statistic (ES). More importantly, to get a clear knowledge of the multiplexing gain of the $3\times3$ MIMO channel, the capacity gain (CG) are computed, which is defined as the channel capacity obtained by the tri-polarized MIMO system over the uni-polarized one. Results of those parameters tell us that, in the same propagation scenario, polarization rotation and coupling performances of the multi-polarized MIMO system have big differences for different layouts of the antenna, correlations between the signals received by two antennas depend on the polarization and orientation of the antenna, and also strongly on the richness of multipath components. In RC and the Hall, for both vertical (Ver) and horizontal (Hor) antenna orientations, and also for the Hor case in office, the maximum CGs are very close to 3, and the mean values are about 2.5, thus 3 independent subchannels can be obtained by this co-located tri-polarized antenna. Furthermore, in office and corridor, for Ver orientation and small distance, the CG will be smaller, however, compared with that in RC, the maximum values of CG get a reduction of 15.5% for the worst case of communication distance equaling to 0.5 m. The results show that the behavior of a multi-polarized MIMO system depends heavily on the polarimetric radiation characteristics of the Tx and Rx antennas, and also on the interactions between the antenna and its operation environment.

The contributions of this paper can be summarized as follows. (1) Channel measurements with respect to compact and planar colocated tri-polarized antenna at both Tx and Rx ends in various multipath scenarios have been conducted, (2) The measured results of channel parameters such as XPD and Ricean K-factor with both communication ends using colocated tri-polarized antennas in RC and practical environments have not been reported before, (3) A very high CG with mean values larger than 2.57 have been got in an OLOS environment with the TX and Rx separated by a pillar, resulted from the rich diffuse scattering, (4) High CC will generally lead to a lower MIMO capacity, however, the negative effect has not been so severe in those scenarios.

## II. MIMO CHANNEL MEASUREMENT SETUP

Extensive measurements are carried out in the ninth floor of the Main building of the Communication University of China. These scenarios include a RC and also some realistic indoor propagation conditions, containing an office room, a corridor and a hall. The dominant building material is reinforced concrete, the walls and floors are made of brick and plaster. For the measurements in office and corridor, there is no obstacles between the Tx and Rx sides, thus a strong LOS signal exists, on the contrary, in the hall, an OLOS case is considered, in which the Tx and Rx antennas are separated by a rectangular pillar. To ensure the statistical stationarity of the propagation, the environment is kept constant with no personnel movement during the measurement.

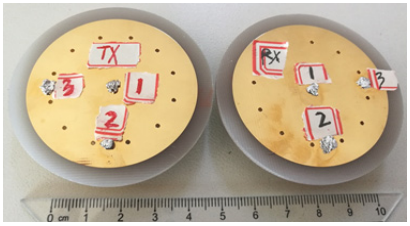


**FIGURE 1.** Photograph of the fabricated antenna.

In each scenario, the measurement system consists of a vector network analyzer (VNA), RF cables, a computer, and the fabricated tri-polarized Tx and Rx antenna, as shown in Fig. 1. The antennas are connected to the VNA by RF cables, the system is thoroughly calibrated and the VNA records the real-time scattering parameters. Then the computer saves and processes the data. The VNA was set to 201 frequencies sweep sample points, a bandwidth of 200 MHz over the working frequency range of the antenna from 3.4 to 3.6 GHz. The noise floor of the VNA is lower than $-90$ dB during the measurement. The transmit power of VNA is set to 0 dBm in the test in the RC, office room and corridor, and it is set to 10 dBm in the test in the hall to get a sufficiently high signal-to-noise ratio (SNR).

### A. EXPERIMENT IN THE RC

In RC, a uniform and statistically repeatable multipath environment can be generated artificially, which can be used to emulate Rayleigh and Ricean-fading environments [22], [23]. Thus, it provides us a very suitable laboratory-produced environment to measure the performance of a MIMO system. The RC used in the measurement has a volume of $1.1 \times 0.7 \times 0.6$ m$^3$ with two metal stirrers [8], which is depicted in Fig. 2. The two stirrers were installed on the bottom of the RC along the $z$ axis with the same dimensions of $0.32 \times 0.2$ m$^2$ and heights of 15 cm and 44 cm, respectively. The mechanical engine of the stirrers can be rotated around a vertical axis ($z$ axis) simultaneously. During the measurement, for each Tx and Rx antenna pair, the two stirrers were rotated from $0^\circ$ to $360^\circ$, with $10^\circ$ increments. Then, this measurement procedure is repeated for different combinations of each $\mathrm{Tx}_i$ and $\mathrm{Rx}_j$ $(i, j = 1, 2, 3)$, with exactly the same stirrer position, so as to guarantee the field environment is repeated exactly for each Tx and Rx antenna pair. Thus, $36 \times 201 = 7236$ samples can be measured for each channel transfer function.

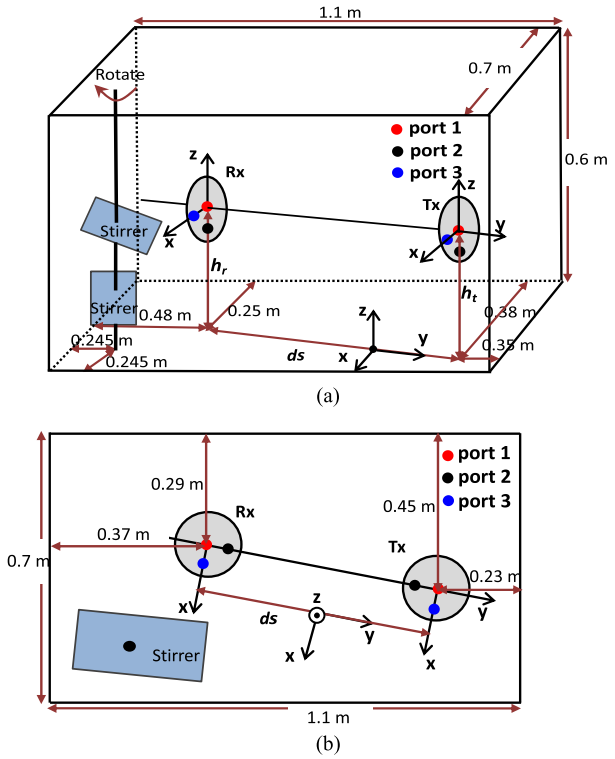


**FIGURE 2.** Measurement in the RC. (a) Side view of the Vertical antenna orientation. (b) Top view of the horizontal antenna orientation.

All the statistical analysis of the channel parameters is based on these samples of the measured channel matrix. Two kinds of placements of the antennas in the measurements are considered. In case 1, as shown in Fig. 2 (a), which is called a Ver orientation, both the Tx and Rx antennas are placed vertically to the bottom of RC. The designed antenna was used with a separation of $d_s = 0.295$ m, and with equal heights of $h_t = h_r = 0.2$ m above the bottom of RC. In case 2, as shown in Fig. 2 (b), which is called a Hor orientation, the antennas were placed horizontally to the bottom of the RC. The two antennas are fixed at a height of $h_t = h_r = 0.27$ m with a separation of $d_s = 0.55$ m. In both of case 1 and case 2, port 1 is located on the origin of the coordinates, for case 1, the Tx and Rx antennas are located on the *xoz* plane, with port 2 located on axis -*z* and port 3 located on axis *x*; for case 2, the Tx and Rx antennas are fixed on the *xoy* plane, with port 2 on axis *y* and port 3 on axis *x*.

### B. EXPERIMENT IN THE OFFICE ROOM

As depicted in Fig. 3, the office room used in our test has the dimensions of $8.6 \times 5.2 \times 3.2$ m$^3$, which consists of some wooden desks, chairs, computers and metal shelves. There are two wooden doors and three glass windows, which are kept closed during the measurements. In case 1, the Tx and Rx are mounted at 1 m above the floor with separation of $d_s = 0.5$ m and 2 m, respectively. In case 2, the height of Tx antenna $h_t$ is 1 m and Rx antenna $h_r$ is 0.79 m, and the separation keeps the same with that of case 1. In both cases,

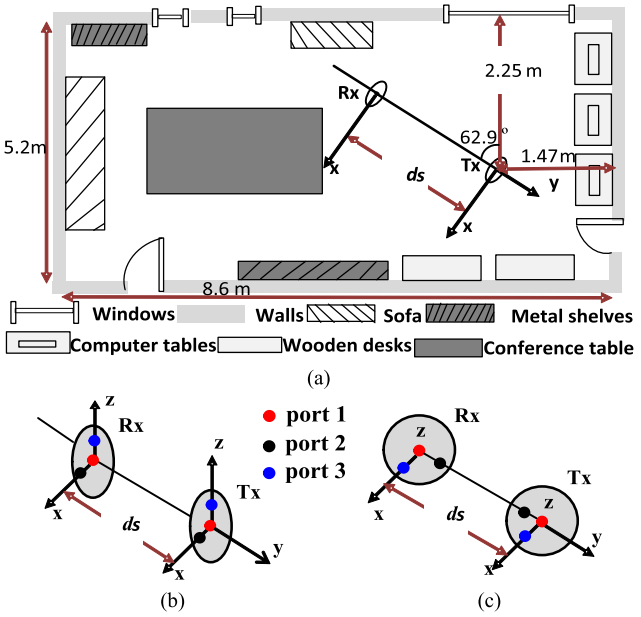


**FIGURE 3.** Measurement in the office. (a) Layout of the room and the antenna. (b) Vertical antenna orientation. (c) Horizontal antenna orientation.

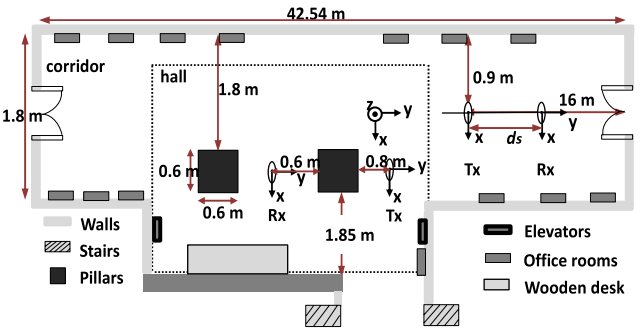


**FIGURE 4.** Measurement in the corridor and the hall.

vertical and horizontal antenna orientations are considered, as shown in Fig. 3 (b) and (c), individually. The positions for the Tx and Rx are randomly selected in the room. During the measurement, the Tx antenna is fixed, and the Rx antenna is moved randomly in 25-30 locations inside a circle with a radius of $\lambda/2$ to catch the small scale fading characteristic of the multipath environment, where $\lambda$ is the wavelength in free space at 3.5 GHz.

### C. EXPERIMENT IN THE CORRIDOR AND HALL

Another measured propagation environment is a rectangular corridor, which has a length of 42.54 m, a width of 1.8 m and a ceiling height of 2.53 m, as shown in Fig. 4. There are two rectangular pillars in the hall.

During the test the position of the Tx antenna is fixed, two placement strategies of the Rx antenna are designed with $d_s = 0.5$ m and 2 m, respectively. The Tx and Rx antennas are placed at the middle of the corridor with the same height of 1 m and with vertical orientations. In the hall, to get an OLOS environment, the Tx and Rx antennas are placed on the

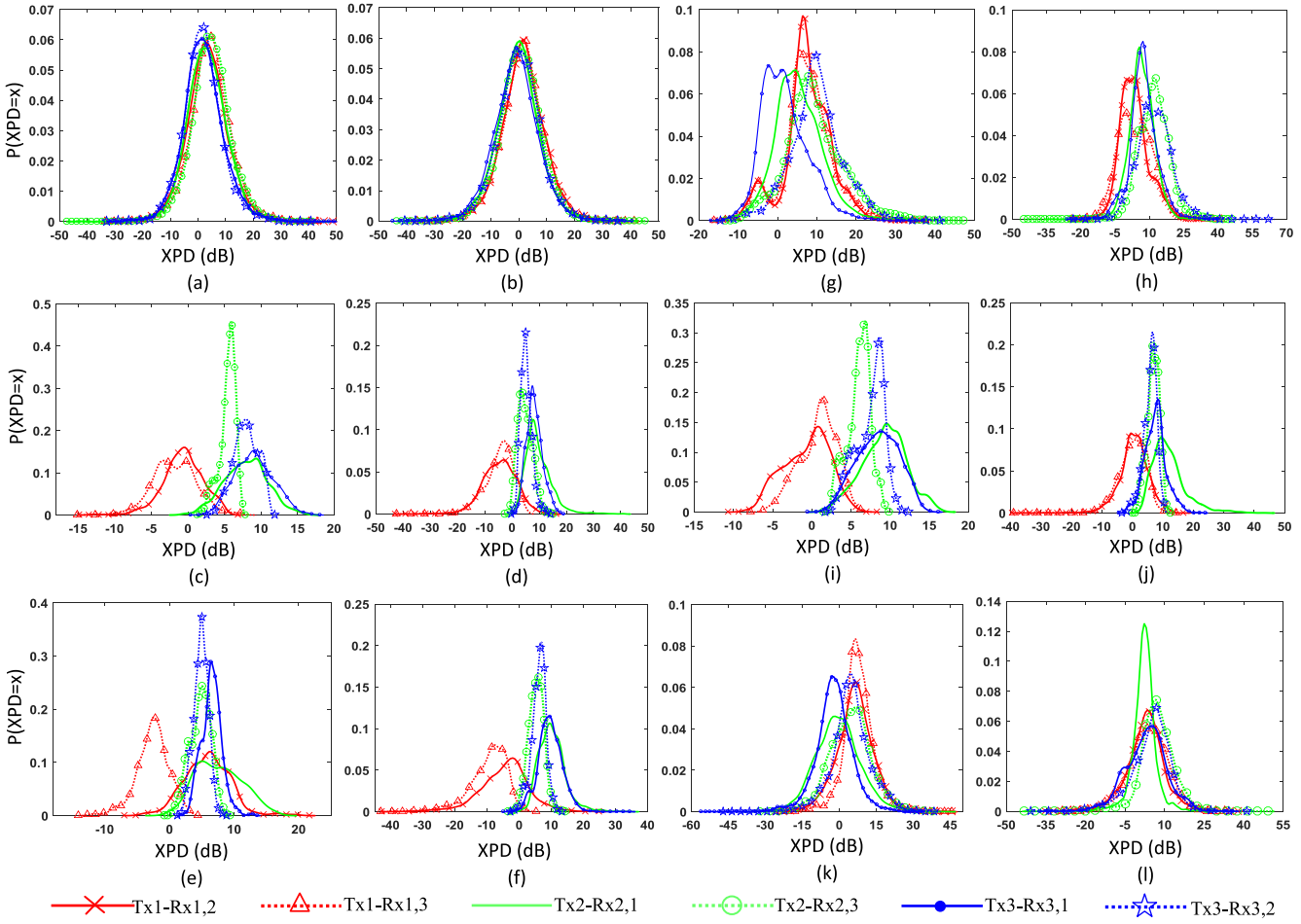


**FIGURE 5.** PDF of XPD in Rx end. (a) RC-Ver. (b) RC-Hor. (c) Office-ds0.5m-Ver-hr1m. (d) Office-ds2m-Ver-hr1m. (e) Office-ds0.5m-Ver-hr79cm. (f) Office-ds2m-Ver-hr79cm. (g) Office-ds0.5m-Hor-hr1m. (h) Office-ds2.0m-Hor-hr1m. (i) Corridor-ds0.5m-Ver-hr1m. (j) Corridor-ds2.0m-Ver-hr1m. (k) Hall-ds2m-Ver-hr1m. (l) Hall-ds2m-Hor-hr1m.

opposite sides of one pillar with separation of 2 m, as shown in Fig. 4. The $h_t = h_r = 1$ m, orientations similar to that in Figs. 3 (b) and (c) are also considered. The measurement procedures in the corridor and the hall are similar to that performed in the office.

## III. PERFORMANCE OF THE TRI-POLARIZED MIMO SYSTEMS

### A. XPD PROPERTIES OF THE MIMO CHANNEL

The XPD property is very important for a multi-polarized wireless channel, which reflects the polarization rotation and coupling caused by propagation environment. Many measurements for the XPD of dual-polarized channels can be found in literature [24]–[27], however, the XPD results related to the tri-polarized antenna is still so few. For a single polarized Tx antenna and a tri-polarized Rx antenna, the XPD and CC were calculated using the measured data for an on-body channel at 2.45 GHz [28]. In addition, for a dual-polarized Tx antenna and a tri-polarized Rx antenna made of three perpendicular monopoles, the XPD performance was investigated in an indoor non-LOS scenario at 3.6 GHz [29]. Although some efforts have been made above, the measured XPD performance for tri-polarized antenna used in both Tx and Rx ends has not been reported.

The XPD is defined as the power imbalance between different polarized Rx or Tx antennas, and for a multi-polarized MIMO system, both the XPD values considering the Tx and Rx ends should be evaluated. For Tx $i$, the XPD between Rx $i$ and $j$ can be expressed as

$$\mathrm{XPD}_{\mathrm{Tx}i-\mathrm{Rx}i,j}(\mathrm{dB}) = 10\left(\log_{10}|h_{ii}|^2 - \log_{10}|h_{ji}|^2\right), \quad (1)$$

where $h_{ij}$ $(i, j = 1, 2, 3, i \neq j)$ is the channel transfer function between the $j$th Tx antenna and the $i$th Rx antenna. Similarly, for Rx $i$, the XPD between Tx $i$ and $j$ can be expressed as

$$\mathrm{XPD}_{\mathrm{Rx}i-\mathrm{Tx}i,j}(\mathrm{dB}) = 10\left(\log_{10}|h_{ii}|^2 - \log_{10}|h_{ij}|^2\right). \quad (2)$$

According to (1) and (2), the probability density functions (PDFs) of XPD can be calculated directly from the measured channel matrix, which are illustrated in Fig. 5. For each of the statistical distributions, it is the analysis over all the random realizations. For an example, in RC, for each measured frequency point, there are totally 36 random realizations for each $h_{ij}$, thus the XPDs based on (1) and (2)

**TABLE 1.** Mean and standard deviation of XPD in Rx end (in dB).

| | $Tx_1$-$Rx_{1,2}$ | | $Tx_1$-$Rx_{1,3}$ | | $Tx_2$-$Rx_{2,1}$ | | $Tx_2$-$Rx_{2,3}$ | | $Tx_3$-$Rx_{3,1}$ | | $Tx_3$-$Rx_{3,2}$ | |
|---|---|---|---|---|---|---|---|---|---|---|---|---|
| | Mean | Std. | Mean | Std. | Mean | Std. | Mean | Std. | Mean | Std. | Mean | Std. |
| RC-Ver | 3.37 | 7.46 | 4.56 | 7.49 | 3.09 | 7.42 | 4.70 | 7.21 | 1.97 | 7.39 | 1.78 | 7.14 |
| RC-Hor | 1.54 | 7.78 | 1.59 | 7.73 | -0.17 | 7.75 | 0.67 | 7.65 | -0.96 | 7.95 | 0.09 | 7.82 |
| Office-Ver-ds0.5m-hr1m | -0.66 | 2.77 | -1.82 | 3.02 | 7.93 | 2.93 | 5.44 | 1.09 | 9.03 | 2.64 | 7.94 | 1.64 |
| Office-Ver-ds2.0m-hr1m | -4.63 | 6.31 | -4.80 | 5.54 | 9.73 | 4.94 | 4.81 | 2.67 | 8.28 | 2.86 | 5.23 | 1.99 |
| Office-Ver-ds0.5m-hr79cm | 5.81 | 3.55 | -2.59 | 2.51 | 7.68 | 3.59 | 4.75 | 1.62 | 6.50 | 1.55 | 4.89 | 1.09 |
| Office-Ver-ds2.0m- hr79cm | -4.53 | 7.61 | -9.73 | 6.01 | 10.28 | 4.15 | 5.28 | 2.30 | 9.68 | 3.74 | 6.15 | 2.15 |
| Office-Hor-ds0.5m-hr1m | 7.40 | 6.28 | 7.33 | 6.58 | 5.51 | 6.50 | 9.38 | 7.47 | 1.85 | 5.83 | 9.86 | 6.60 |
| Office-Hor-ds2.0m-hr1m | 3.43 | 6.26 | 4.08 | 7.70 | 6.70 | 5.42 | 11.78 | 6.86 | 7.47 | 6.22 | 12.20 | 7.49 |
| Corridor-Ver-ds0.5m-hr1m | -0.71 | 2.91 | 0.78 | 2.37 | 9.23 | 2.81 | 6.00 | 1.44 | 8.42 | 2.63 | 7.45 | 1.80 |
| Corridor-Ver-ds2.0m-hr1m | 0.42 | 4.96 | -0.05 | 4.67 | 12.03 | 5.64 | 6.85 | 1.97 | 7.55 | 3.56 | 5.78 | 2.19 |
| Hall-Ver-ds2.0m-hr1m | 6.33 | 7.67 | 7.77 | 6.23 | -0.54 | 9.01 | 4.54 | 8.45 | -2.15 | 7.46 | 4.84 | 7.88 |
| Hall-Hor-ds2.0m-hr1m | 2.68 | 7.61 | 3.73 | 7.24 | 2.17 | 4.78 | 7.29 | 6.48 | 2.95 | 7.79 | 4.92 | 7.64 |

can be computed, then they are statistical analyzed over all the 36 realizations and over the working bandwidth.

Results in Fig. 5 tell us that, in RC, the PDFs of XPD are very close to normal distributed functions, and for different Tx and Rx ports, they have a very high degree of consistency. However, in office and corridor, the PDF results have some deviations from the normal distribution. More interestingly, the results in hall are very close to that in RC. For all the scenarios, the PDFs of the Tx end are very similar to that of the Rx end, which are thus not presented here. Physically, the results can be explained that, RC is an isotropic and randomly polarized scattering scenario, which can give very uniform impact on different polarized incoming signals, thus, the polarization coupling effects for different polarizations are similar. However, in the office and indoor environments, there are some sparse multipath reflections mainly from the ground and walls, which have different effects on different incident polarizations, thus, there are big differences in the PDFs of XPD for different polarizations. In the hall, since the Tx and Rx are separated by a pillar which obstructed the signals in the first Fresnel region, thus a very typical OLOS environment was formulated. Surprisingly, the XPD results in this scenario are very close to that in RC, maybe because of the rich diffuse scattering produced by the edges of the pillar.

In addition, Table 1 presents the mean value and standard deviation (Std.) of XPD computed from the PDFs in Fig. 5. It can be seen that, compared with other scenarios, in RC, the absolute values of mean XPD are the smallest, however, the Stds. of XPD are almost the largest, larger than 7 dB. The large spread of XPD means that sometimes the power received by co-polarized antenna are larger than that received by the cross-polarized one, and sometimes it is on the contrary, but the possibilities of the two cases are almost the same, thus the mean values are close to zero.

In office and corridor, the most prominent feature is that, for Tx 1, with Ver orientation, almost all the means of XPD are negative, but with Hor orientation, the means of XPD are all positive. This phenomenon means that there is a very strong polarization rotation and a high cross-polarization coupling when the monopole is parallel to the ground, but the polarization is well maintained when it is vertical to the ground. This could be explained from the theory of image source that, for the parallel monopole, the ground and ceiling will produce image sources with opposite phases to that of original source, which will weaken the signal of co-polarization, but for the vertical monopole, the image sources will have the same phase with that of original source, which will enhance the signal of co-polarization. Moreover, the walls and the furniture will also produce some multi-path signals, but the antennas are more close to the ground, so it has the largest contribution. Thus, we can see that, in the same propagation scenario, big difference will exist in the polarization rotation and coupling performances of the multi-polarized MIMO system for different layouts of the antenna.

### B. RICEAN K-FACTOR

In wireless communications, the time-varying magnitude of the channel gain was generally represented by a Ricean distributed function [30]. The key parameter of the first-order statistics of this distribution is the Ricean $K$-factor, which is the power ratio of the direct and scattered components of the received signal. The $K$-Factor provides a useful measure of the link quality to characterize the channel of SISO system [31]. Furthermore, for a MIMO system, it has been verified that there are some relationships between Ricean $K$-Factor and the spatial correlation properties of the channel responses [32], and thus it has big impact on the capacity of a MIMO channel.

Here, the $K$-factor is estimated from the measured transfer function of each MIMO channel using the method presented in [31] [33]. For channel response $h_{ij}$, it could be

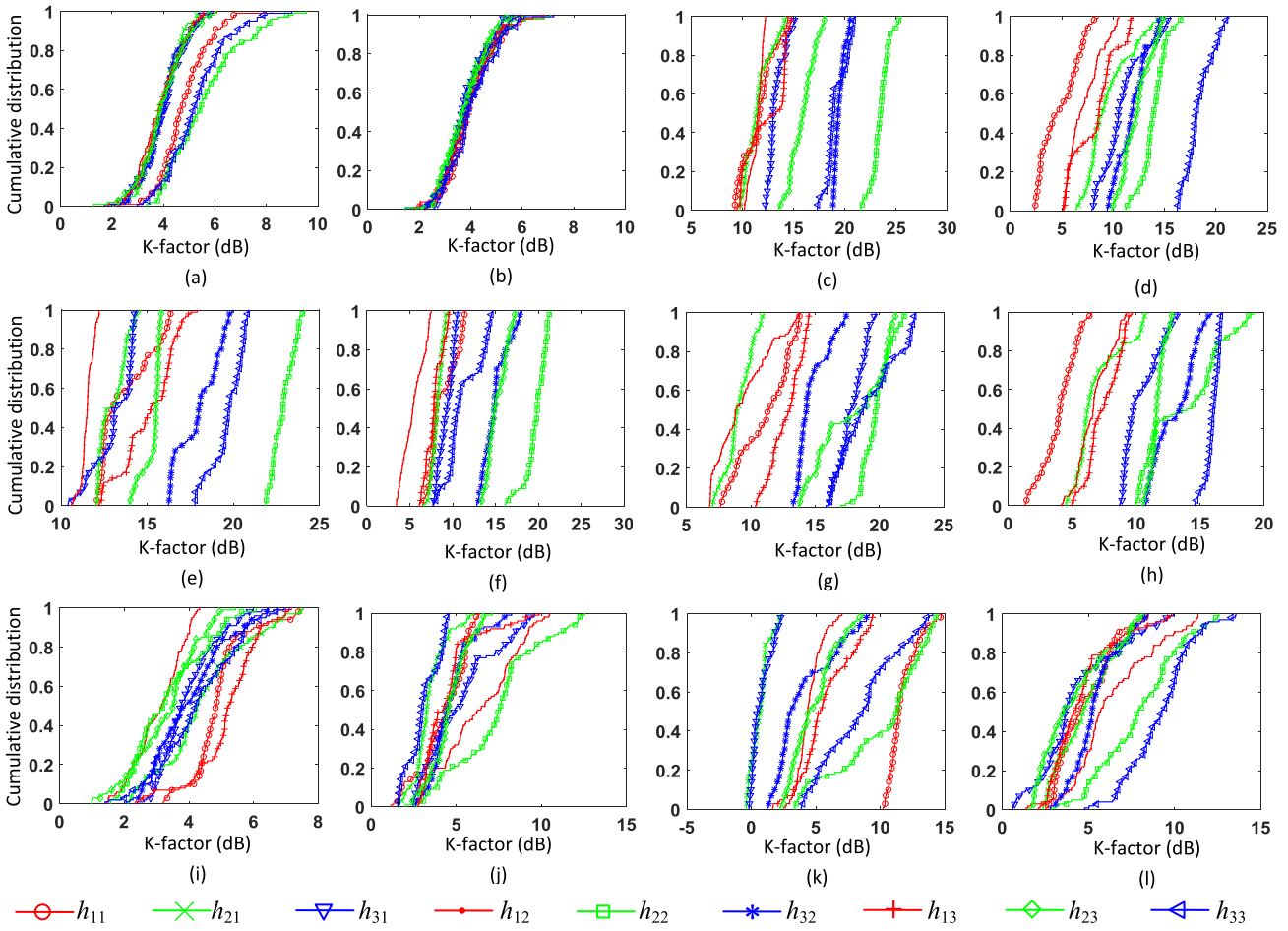


**FIGURE 6.** Cumulative distribution of XPD in different scenarios. (a) RC-Ver. (b) RC-Hor. (c) Office-ds0.5m-Ver-hr1m. (d) Office-ds2.0m-Ver-hr1m. (e) Corridor-ds0.5m-Ver-hr1m. (f) Corridor-ds2.0m-Ver-hr1m. (g) Office-ds0.5m-Ver-hr79cm. (h) Office-ds2.0m-Ver-hr79cm. (i) Hall-ds2m-Ver-hr1m. (j) Hall- ds2m-Hor-hr1m. (k) Office-ds0.5m-Hor-hr1m. (l) Office-ds2.0m-Hor-hr1m.

expressed as,

$$\mathrm{K\,(dB)} = E\left[|h_{ij}|\right]^2 / 2Var\left(|h_{ij}|\right), \tag{3}$$

where $E$ and $Var$ denote the calculation of expectation and variance, respectively.

The cumulative distribution functions (CDFs) of $K$-factor for each element of the MIMO channel matrix are given in Fig. 6. We can see that, for all the scenarios, the values of $K$-factor in RC are the smallest, between 1-9 dB, which means the scattered signals have the largest contribution. The results in hall are also very close to that in RC, which is caused by the diffuse scattering produced by the edges of the column. For the Ver antenna layout, in the office and corridor, the $K$-factors are obviously larger than that in RC and hall, moreover, the results are not consistent for different polarizations. In addition, we can see that, when $d_s$ is increased from 0.5 m to 2.0 m, the $K$-factors will have an obvious reduction, which is caused by the enhancing of the contribution of the scattering components in the total received signal.

### C. CORRELATION COEFFICIENT

Many efforts have been made to investigate the relationship between spatial correlation and the MIMO capacity, using the measured data by different antennas in various propagation conditions. It has been demonstrated that signal correlation could limit the achievable capacity of MIMO systems [34]–[36]. Using cavity backed slot antenna arrays separated by $\lambda/2$ in an indoor environment, the MIMO capacities have been shown to decrease with an increased spatial correlation [34]. It was verified that the spatial correlation in LOS scenario is obviously larger than that in NLOS scenario in an office, which caused a sharp decrease in MIMO capacity, using a uniform linear array of four $\lambda/4$ monopoles [35]. Furthermore, the spatial correlation could be increased and cause a reduced average MIMO capacity with increasing of Ricean $K$-factor [36]. However, it has also been stated that [37]–[39], although it is always true that low correlation will lead to better performance of a MIMO system, high correlation is not necessarily producing noticeably worse performance, with emphasis on MIMO antenna in small terminals.

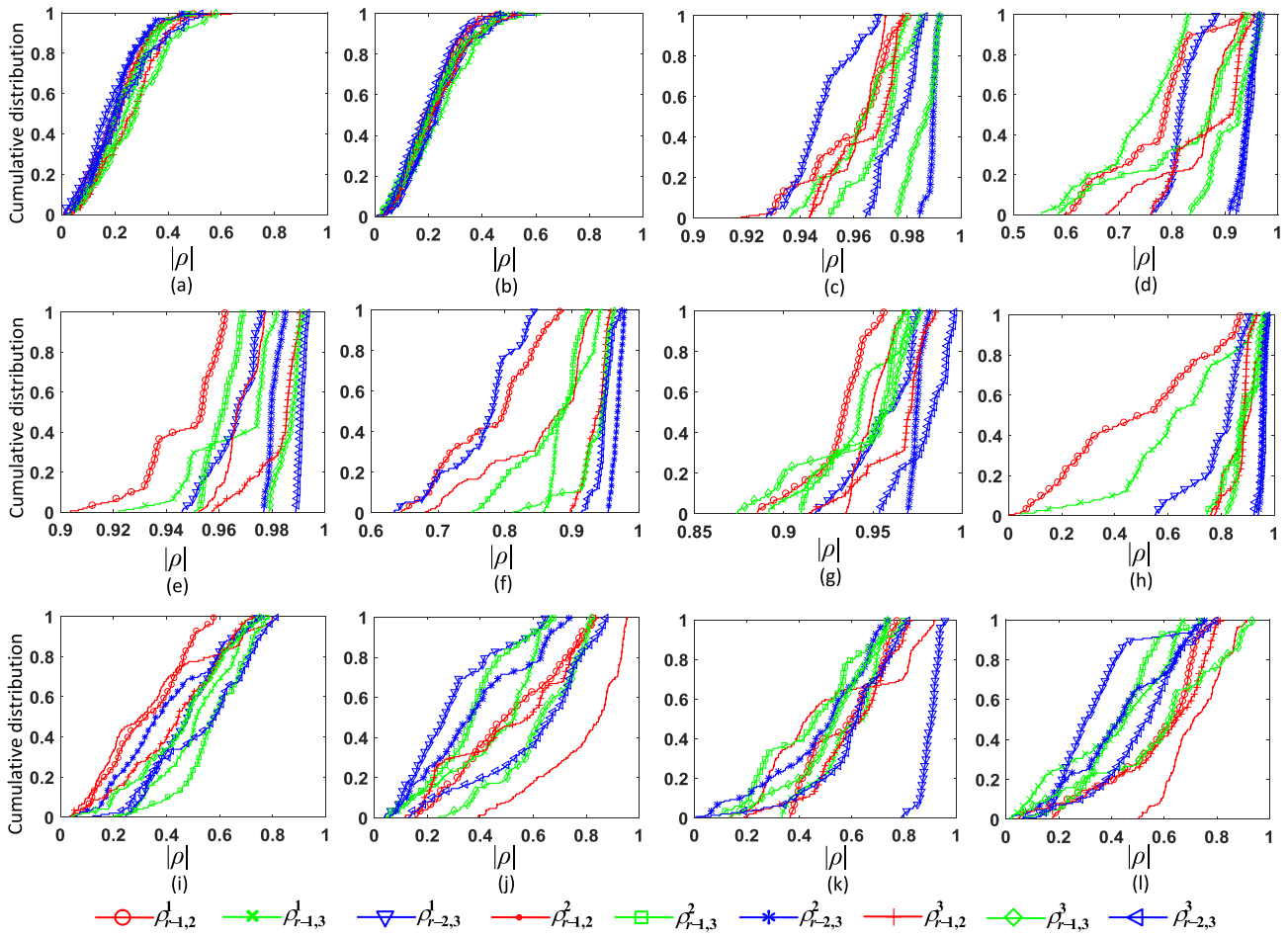


**FIGURE 7.** CC in different scenarios of Rx end. (a) RC-Ver. (b) RC-Hor. (c) Office-ds0.5m-Ver-hr1m. (d) Office-ds2.0m-Ver-hr1m. (e) Corridor-ds0.5m-Ver-hr1m. (f) Corridor-ds2.0m-Ver-hr1m. (g) Office-ds0.5m-Ver-hr79cm. (h) Office-ds2.0m-Ver-hr79cm. (i) Hall-ds2m-Ver-hr1m. (j) Hall- ds2m-Hor-hr1m. (k) Office-ds0.5m-Hor-hr1m. (l) Office-ds2.0m-Hor-hr1m.

The complex CC for two complex random variables $u$ and $v$ is defined as

$$\rho_{\text{complex}} = \frac{E\left[uv^*\right] - E[u]E[v^*]}{\sqrt{\left(E\left[|u|^2\right] - |E\left[u\right]|^2\right)\left(E\left[|v|^2\right] - |E\left[v\right]|^2\right)}}, \tag{4}$$

where $^*$ denotes the complex conjugate operation.

When individual channels are correlated, the covariance matrix $\mathbf{R}$ should be investigated to get a comprehensive understanding of the statistical performance of $\mathbf{H}$, which can be calculated as

$$\mathbf{R} = E\left\{vec(\mathbf{H})vec(\mathbf{H})^{\dagger}\right\}, \tag{5}$$

where $\mathbf{H}^{\dagger}$ means the transpose conjugate of $\mathbf{H}$ and $vec\ (\mathbf{H})$ is the operator stacking the matrix $\mathbf{H}$ into a column-wise vector. For the $3 \times 3$ MIMO system, $\mathbf{R}$ should be a matrix of $9 \times 9$.

We study the correlation properties of $\mathbf{H}$ in Tx side and Rx side, individually. The CC in Rx end $\rho^l_{r-i,j}$ means the correlation between the $i$-th and $j$-th Rx antenna elements, with respect to the $l$-th Tx antenna; similarly, the CC in Tx end $\rho^l_{t-i,j}$ means the correlation of the signals received by the $l$-th Rx antenna, arriving from the $i$-th and the $j$-th Tx antenna elements. For all the scenarios, the CC results of the Tx end are very similar to that of the Rx end, which are not presented here.

Based on (4), firstly, for each frequency point the CC is calculated considering the statistical realizations of the channel, for an example, 36 samples in RC, then, the CDF can be obtained based on statistical analysis over the measured frequency band. The CDF curves of $|\rho|$ are charted in Fig. 7. We can see that for various polarizations, the statistical properties of correlation amplitude are almost the same in RC, however, in other scenarios, they have obvious differences. Furthermore, for both the Ver and Hor antenna orientations, the correlations in RC are the smallest. In office and corridor, for Ver orientation, the CCs are very big for $d_s = 0.5$ m, however, when it is increased to 2.0 m, it will get an evident reduction. The results in Fig. 7 could be explained that, the CC of two received signals is mainly affected by the

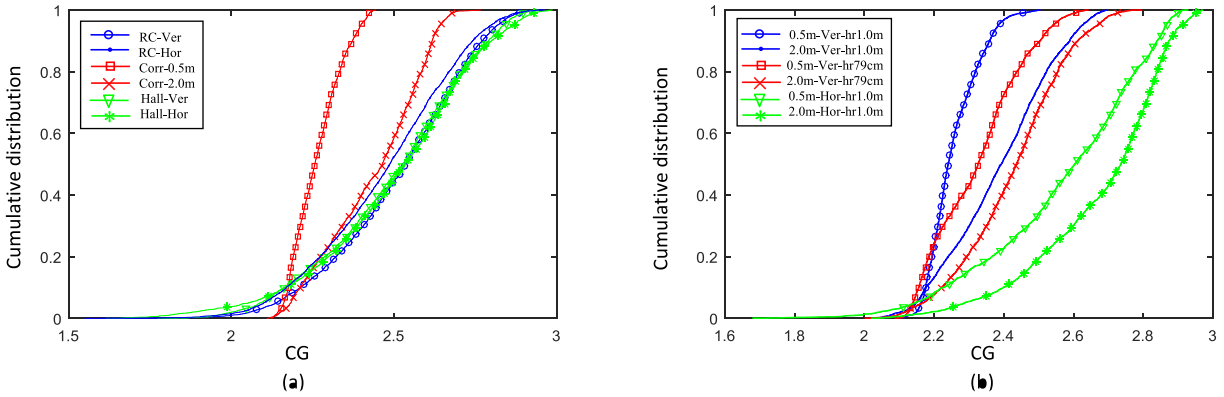


**FIGURE 8.** Channel capacity gain in various scenarios. (a) RC, corridor and hall. (b) Office.

**TABLE 2.** Maximum and mean CG in various scenarios.

| Scenarios | RC-Ver | RC-Hor | Corr-0.5m | Corr-2.0m | Hall-Ver | Hall-Hor | Offi-Ver-0.5m-hr1m | Offi-Ver-2m-hr1m | Offi-Ver-0.5m-hr79cm | Offi-Ver-2m-hr79cm | Offi-hor-0.5m-hr1m | Offi-hor-2m-hr1m |
|---|---|---|---|---|---|---|---|---|---|---|---|---|
| MAX | 2.96 | 2.96 | 2.44 | 2.77 | 2.95 | 2.99 | 2.50 | 2.70 | 2.64 | 2.80 | 2.93 | 2.97 |
| MEAN | 2.51 | 2.47 | 2.26 | 2.44 | 2.50 | 2.50 | 2.26 | 2.39 | 2.32 | 2.43 | 2.57 | 2.68 |

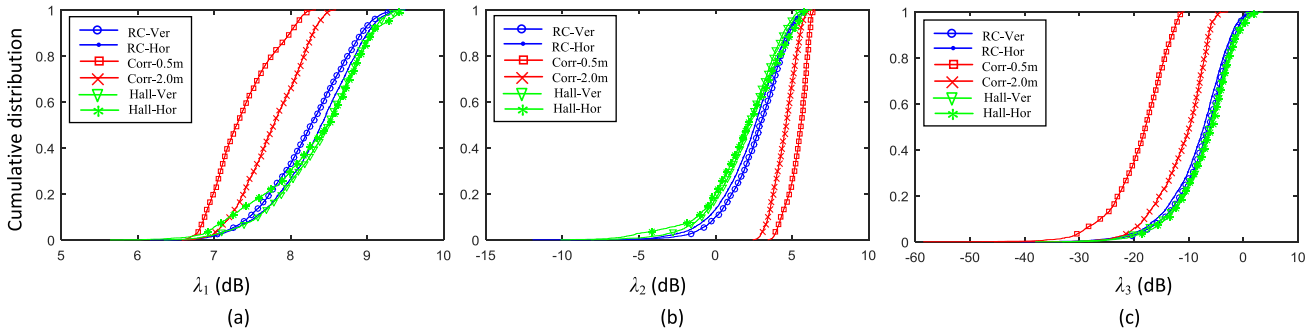


**FIGURE 9.** Eigenvalues of channel matrix in RC, corridor and hall. (a) $\lambda_1$. (b) $\lambda_2$. (c) $\lambda_3$.

richness of the multipath between the Tx and Rx, there are very rich multipath propagations in RC and OLOS case in the hall, thus a very small correlation exists between the channel transfer functions. In the office and corridor, for Ver antenna layout, when $d_s = 0.5$ m, the main received signal is from the direct path, corresponding to a very large correlation and also a large Ricean $K$-factor, with the increase of communication distance, the contributions of reflection and scattering will be enhanced and lead to the reducing of correlation and $K$-factor. However, for the Hor antenna case, the richness of multipath in office and corridor are sufficiently enough for various communication distances, thus a low correlation and $K$-factor can be obtained.

### D. CHANNEL CAPACITY

The capacity is computed by the widely used expressions for MIMO capacity calculation with equal transmit power over each transmit antenna [40], which approaches to the performance of the water-filling power allocation for high SNR,

$$C = \log_2 \det(\mathbf{I} + (SNR/n_T)\mathbf{H}\mathbf{H}^{\dagger})(\text{bps/Hz}), \quad (6)$$

where $\mathbf{I}$ is $3 \times 3$ identical matrix, $n_T = 3$. A widely used channel normalization is adopt, $\|\mathbf{H}\|_F^2 = n_T n_R$, where $\|\cdot\|_F$ denotes the Frobenius norm. By this normalization, the effect of the absolute value of the received power on the MIMO capacity was removed, thus the impacts of the multipath richness of the environment can be well illustrated. Here, we assume a 20 dB SNR and the CG obtained by the tri-polarized MIMO system over the uni-polarized one is computed.

In Fig. 8 the CDFs of the $3 \times 3$ tri-polarized MIMO CG are illustrated. Fig. 8 (a) tells us that for both the Ver and Hor antenna orientations, in RC, large MIMO capacity gain can be obtained by the colocated tri-polarized antenna, and the CGs in the hall are very close to that in RC. In the case of corridor, for $d_s = 0.5$ m, the CG is obviously smaller than that in RC, however, for $d_s = 2.0$ m, the CG will get a big increase and close to that in RC. Fig. 8 (b) shows that, in the office, the CGs of Ver orientation are evidently smaller than that of Hor case, moreover, similar to the case in corridor, when $d_s$ is increased from 0.5 m to 2.0 m, the CG will be greatly increased in office

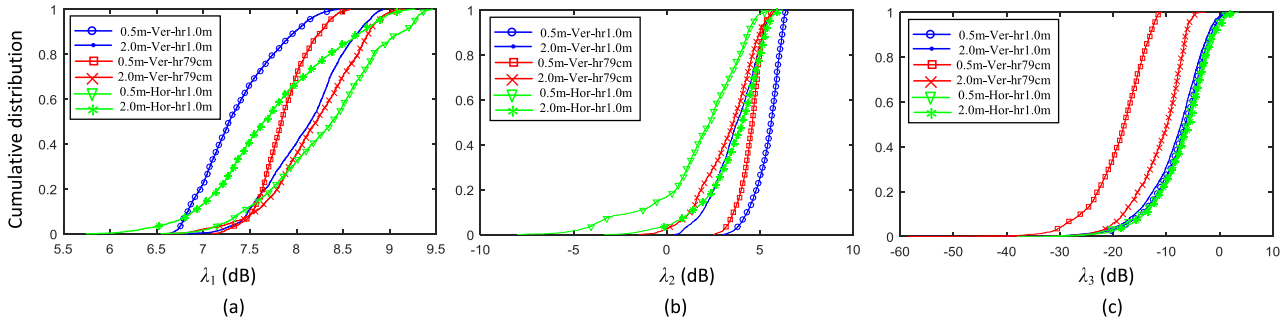


**FIGURE 10.** Eigenvalues of channel matrix in office. (a) $\lambda_1$. (b) $\lambda_2$. (c) $\lambda_3$.

for both the Ver and Hor orientations. The differences of CG in various scenarios can be well explained from the results of CC, and we can see that a smaller CC will generally result in a larger CG. Moreover, the maximum and mean values of CG in those scenarios have also been computed and listed in Table 2, which tells us that, in RC and the hall, for both Ver and Hor orientations, and also for the Hor case in office, the maximum CGs are very close to 3, larger than 2.9 and the mean CGs are about 2.5, thus 3 independent subchannels can be obtained by this co-located tri-polarized antenna. It can also be seen that, in office and corridor for Ver orientation and small distance, the CG will be smaller, however, compared with that in RC, the maximum CGs get a reduction of 15.5% and its mean values are reduced only 9.9% for the worst case of $d_s = 0.5$ m in office and corridor. Considering that the CCs in those cases are very high, with the mean values larger than 0.9, thus we can see that the high CC will generally lead to a lower MIMO capacity, however, the negative effect is not so severe in those case.

### E. EIGENVALUE OF CHANNEL MATRIX

To get a deeper understanding of the CG results in various scenarios, we can also do the singular value decomposition (SVD) [41] for the channel matrix $\mathbf{H}$. Through SVD, $\mathbf{H}$ can be decomposed into a set of eigen channels each corresponding to a singular value, the squared singular values, are called eigenvalues of $\mathbf{HH}^{\dagger}$, denoted as, $\lambda_1, \lambda_2, \ldots, \lambda_M$ where $M$ is the rank of $\mathbf{H}$, and the channel capacity can also be expressed as

$$C = \sum_{i=1}^{M} \log_2 \left(1 + \left(SNR/n_T\right)\lambda_i\right). \tag{7}$$

Thus, by (7) the contribution of each eigenvalue to the overall MIMO capacity can be clearly illustrated. In Fig. 9 and Fig. 10, the CDFs of the eigenvalues of the channel matrix in various scenarios are described. Results show that in all the cases, three non-zero eigenvalues can be obtained, which also indicates that three independent subchannels can be supported.

### F. CHANNEL ELLIPTICITY STATISTIC

Channel ES is a measure for multipath richness [42] [43], which indicates the capability of spatial multiplexing in a MIMO antenna system. The ES of a MIMO channel is defined as the ratio of the geometric mean $m_g$ and the arithmetic mean $m_a$ of eigenvalues of $\mathbf{HH}^{\dagger}$ and can be written as [42]

$$ES = m_g/m_a = \left(\prod_{k=1}^{M} \lambda_k\right)^{\frac{1}{M}} / \frac{1}{M}\sum_{k=1}^{M} \lambda_k. \tag{8}$$

As can be seen from (8), the value of $ES$ is 0 if one of the eigenvalues is zero, which means the multipath is not sufficiently rich to support $M$ parallel modes of communication and the channel is rank deficient. If all eigenvalues are equal, $ES = 1$. The CDFs of ES corresponding to the $3 \times 3$ tri-polarized MIMO channel are given in Fig. 11. Fig. 11 (a)

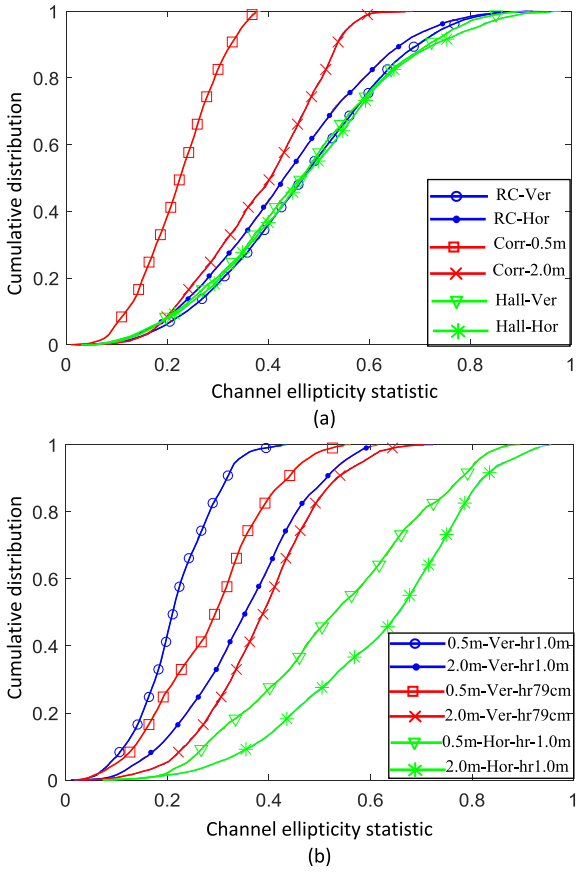


**FIGURE 11.** Channel ellipticity statistic in various scenarios. (a) RC, corridor and hall. (b) Office.

shows that in RC and hall, large MIMO channel ES can be obtained for both the Ver and Hor orientations, however, it decreases significantly in the corridor when the distance $d_s$ is 0.5 m. The result in Fig. 11 (b) illustrates that, in the office, the channel ES results of Ver orientation are evidently smaller than that of Hor case. Furthermore, the ES improves when $d_s$ is increased from 0.5 m to 2.0 m. Fig. 11 tells us that, the channel ES generally increase with the richness of multipath, which is in accordance with the above result of channel CG.

## IV. CONCLUSION

Based on a multi-mode colocated orthogonal tri-polarized antenna, comprehensive measurements are performed in a variety of scenarios with different multipath scatterings, including a RC, an office room, a corridor and a hall. Based on the measured data, the performance of the tri-polarized MIMO system has been analyzed in terms of XPD, Ricean $K$-factor, CC, MIMO CG, and so on. Results show that, for different Tx and Rx ports, in RC, the PDFs of XPD are highly consistent and are very close to normal distributions, however, in office and corridor, the PDF results have some deviations from the normal distribution, and also show heavy dependences on the orientation of the antenna. For the $K$-factor, in RC, they are the smallest, between 1-9 dB, and the distributions for different $h_{ij}$ are more close to each other. The results of XPD and $K$-factor in the OLOS case in the hall are very close to that in RC, which indicates that similar multipath scatterings exit in those environments. In addition, in the office and corridor, the $K$-factors are obviously larger than that in RC and hall for the vertical antenna layout, and the results are not consistent for various ports. More importantly, high CC will generally lead to a lower MIMO capacity; however, the negative effect is not so severe in those cases. Results from this paper can provide an overall understanding of the performance of tri-polarized MIMO system in multipath environment.

## REFERENCES

[1] M. R. Andrews, P. P. Mitra, and R. D. Carvalho, "Tripling the capacity of wireless communications using electromagnetic polarization," *Nature*, vol. 409, pp. 316–318, Jan. 2001.

[2] M. C. Mtumbuka and D. J. Edwards, "Investigation of tri-polarised MIMO technique," *Electron. Lett.*, vol. 41, no. 3, pp. 137–138, Feb. 2005.

[3] B. N. Getu and J. B. Andersen, "The MIMO cube-a compact MIMO antenna," *IEEE Trans. Wireless Commun.*, vol. 4, no. 3, pp. 1136–1141, May 2005.

[4] A. S. Konanur, K. Gosalia, S. H. Krishnamurthy, B. Hughes, and G. Lazzi, "Increasing wireless channel capacity through MIMO systems employing co-located antennas," *IEEE Trans. Microw. Theory Techn.*, vol. 53, no. 6, pp. 1837–1844, Jun. 2005.

[5] D. Piao, "Characteristics of the hexapolarized MIMO channel over free-space and three non-free-space scenarios," *IEEE Trans. Wireless Commun.*, vol. 12, no. 8, pp. 4174–4182, Aug. 2013.

[6] G. Gupta, B. L. Hughes, and G. Lazzi, "On the degrees of freedom in linear array systems with tri-polarized antennas," *IEEE Trans. Wireless Commun.*, vol. 7, no. 7, pp. 2458–2462, Jul. 2008.

[7] C.-Y. Chiu, J.-B. Yan, and R. D. Murch, "Compact three-port orthogonally polarized MIMO antennas," *IEEE Antennas Wireless Propag. Lett.*, vol. 6, pp. 619–622, Dec. 2007.

[8] D. Piao, L. Yang, Q. Guo, Y. Mao, and Z. Li, "Measurement-based performance comparison of colocated tripolarized loop and dipole antennas," *IEEE Trans. Antennas Propag.*, vol. 63, no. 8, pp. 3371–3379, Aug. 2015.

[9] K. Itoh, R. Watanabe, and T. Matsumoto, "Slot-monopole antenna system for energy-density reception at UHF," *IEEE Trans. Antennas Propag.*, vol. AP-27, no. 4, pp. 485–489, Jul. 1979.

[10] D. Gray and T. Watanabe, "Three orthogonal polarisation DRA-monopole ensemble," *Electron. Lett.*, vol. 39, no. 10, pp. 766–767, May 2003.

[11] N. K. Das, T. Inoue, T. Taniguchi, and Y. Karasawa, "An experiment on MIMO system having three orthogonal polarization diversity branches in multipath-rich environment," in *Proc. IEEE 60th Veh. Technol. Conf.*, Sep. 2004, pp. 1528–1532.

[12] H. Zhong, Z. Zhang, W. Chen, Z. Feng, and M. F. Iskander, "A tripolarization antenna fed by proximity coupling and probe," *IEEE Antennas Wireless Propag. Lett.*, vol. 8, pp. 465–467, 2009.

[13] X. Gao, H. Zhong, Z. Zhang, Z. Feng, and M. F. Iskander, "Low-profile planar tripolarization antenna for WLAN communications," *IEEE Antennas Wireless Propag. Lett.*, vol. 9, pp. 83–86, 2010.

[14] Y. Zhang, K. Wei, Z. Zhang, and Z. Feng, "A broadband patch antenna with tripolarization using quasi-cross-slot and capacitive coupling feed," *IEEE Antennas Wireless Propag. Lett.*, vol. 12, pp. 832–835, 2013.

[15] K.-F. Tong, H.-J. Tang, A. Al-Armaghany, and W. Hong, "Low-profile orthogonally tripolarized antennas," *IEEE Antennas Wireless Propag. Lett.*, vol. 12, pp. 876–879, 2013.

[16] N. P. Lawrence, C. Fumeaux, and D. Abbott, "Planar triorthogonal diversity slot antenna," *IEEE Trans. Antennas Propag.*, vol. 65, no. 3, pp. 1416–1421, Mar. 2017.

[17] M.-Y. Li, Y.-L. Ban, Z.-Q. Xu, J. Guo, and Z.-F. Yu, "Tri-polarized 12-antenna MIMO array for future 5G smartphone applications," *IEEE Access*, vol. 6, pp. 6160–6170, 2017.

[18] L. Liu, C. Liu, Z. Li, X. Yin, and Z. N. Chen, "Slit-slot line and its application to low cross-polarization slot antenna and mutual-coupling suppressed tripolarized MIMO antenna," *IEEE Trans. Antennas Propag.*, vol. 67, no. 1, pp. 4–15, Jan. 2019.

[19] D. Piao and Y. Wang, "Tripolarized MIMO antenna using a compact single-layer Microstrip patch," *IEEE Trans. Antennas Propag.*, vol. 67, no. 3, pp. 1937–1940, Mar. 2019.

[20] WRC-15 Press Release, World Radiocommunication Conference. (Nov. 27, 2015). *Allocates Spectrum for Future Innovation*. [Online]. Available: http://www.itu.int/net/pressoffice/press_releases/2015/56.aspx

[21] Y. Li, C.-Y.-D. Sim, Y. Luo, and G. Yang, "12-port 5G massive MIMO antenna array in sub-6GHz mobile handset for LTE bands 42/43/46 applications," *IEEE Access*, vol. 6, pp. 344–354, 2018.

[22] P.-S. Kildal and K. Rosengren, "Correlation and capacity of MIMO systems and mutual coupling, radiation efficiency, and diversity gain of their antennas: Simulations and measurements in a reverberation chamber," *IEEE Commun. Mag.*, vol. 42, no. 12, pp. 104–112, Dec. 2004.

[23] J. D. Sanchez-Heredia, J. F. Valenzuela-Valdes, A. M. Martinez-Gonzalez, and D. A. Sanchez-Hernandez, "Emulation of MIMO Rician-fading environments with mode-stirred reverberation chambers," *IEEE Trans. Antennas Propagat.*, vol. 59, no. 2, pp. 654–660, Feb. 2011.

[24] C. Oestges, V. Erceg, and A. J. Paulraj, "Propagation modeling of MIMO multipolarized fixed wireless channels," *IEEE Trans. Veh. Technol.*, vol. 53, no. 3, pp. 644–654, May 2004.

[25] W. Q. Malik, "Polarimetric characterization of ultrawideband propagation channels," *IEEE Trans. Antennas Propag.*, vol. 56, no. 2, pp. 532–539, Feb. 2008.

[26] V. Degli-Esposti, V.-M. Kolmonen, E. M. Vitucci, and P. Vainikainen, "Analysis and modeling on co- and cross-polarized urban radio propagation for dual-polarized MIMO wireless Systems," *IEEE Trans. Antennas Propag.*, vol. 59, no. 11, pp. 4247–4256, Nov. 2011.

[27] D. P. Gaillot, E. Tanghe, W. Joseph, P. Laly, V.-C. Tran, M. Liénard, and L. Martens, "Polarization properties of specular and dense multipath components in a large industrial Hall," *IEEE Trans. Antennas Propag.*, vol. 63, no. 7, pp. 3219–3228, Jul. 2015.

[28] Y. Yao, J. Zheng, and Z. Feng, "Diversity measurements for on-body channels using a tri-polarization antenna at 2.45 GHz," *IEEE Antennas Wireless Propag. Lett.*, vol. 11, pp. 1285–1288, 2012.

[29] F. Quitin, C. Oestges, F. Horlin, and P. D. Doncker, "Polarization measurements and modeling in indoor NLOS environments," *IEEE Trans. Wireless Commun.*, vol. 9, no. 1, pp. 21–25, Jan. 2010.

[30] L. J. Greenstein, S. S. Ghassemzadeh, V. Erceg, and D. G. Michelson, "Ricean $K$-factors in narrow-band fixed wireless channels: Theory, experiments, and statistical models," *IEEE Trans. Veh. Technol.*, vol. 58, no. 8, pp. 4000–4012, Oct. 2009.
[31] C. Tepedelenlioglu, A. Abdi, and G. B. Giannakis, "The Ricean K factor: Estimation and performance analysis," *IEEE Trans. Wireless Commun.*, vol. 2, no. 4, pp. 799–810, Jul. 2003.
[32] V. Tarokh, N. Seshadri, and A. R. Calderbank, "Space-time codes for high data rate wireless communication: Performance criterion and code construction," *IEEE Trans. Inf. Theory*, vol. 44, no. 2, pp. 744–765, Mar. 1998.
[33] I. B. Mabrouk, J. Hautcoeur, L. Talbi, M. Nedil, and K. Hettak, "Feasibility of a millimeter-wave MIMO system for short-range wireless communications in an underground gold mine," *IEEE Trans. Antennas Propag.*, vol. 61, no. 8, pp. 4296–4305, Aug. 2013.
[34] P. Kyritsi, D. C. Cox, R. A. Valenzuela, and P. W. Wolniansky, "Correlation analysis based on MIMO channel measurements in an indoor environment," *IEEE J. Sel. Areas Commun.*, vol. 21, no. 5, pp. 713–720, Jun. 2003.
[35] P. L. Kafle, A. Intarapanich, A. B. Sesay, J. Mcrory, and R. J. Davies, "Spatial correlation and capacity measurements for wideband MIMO channels in indoor office environment," *IEEE Trans. Wireless Commun.*, vol. 7, no. 5, pp. 1560–1571, May 2008.
[36] I. Khan and P. S. Hall, "Experimental evaluation of MIMO capacity and correlation for narrowband body-centric wireless channels," *IEEE Trans. Antennas Propag.*, vol. 58, no. 1, pp. 195–202, Jan. 2010.
[37] B. Yanakiev, J. Nielsen, M. Christensen, and G. F. Pedersen, "On small terminal antenna correlation and impact on MIMO channel capacity," *IEEE Trans. Antennas Propag.*, vol. 60, no. 2, pp. 689–699, Feb. 2012.
[38] J. N. Pierce and S. Stein, "Multiple diversity with nonindependent fading," *Proc. IRE*, vol. 48, no. 1, pp. 89–104, 1960.
[39] T. Svantesson, "Correlation and channel capacity of MIMO systems employing multimode antennas," *IEEE Trans. Veh. Technol.*, vol. 51, no. 6, pp. 1304–1312, Nov. 2002.
[40] G. J. Foschini and M. J. Gans, "On limits of wireless communications in a fading environment when using multiple antennas," *Wireless Pers. Commun.*, vol. 6, no. 3, pp. 311–335, 1998.
[41] E. Telatar, "Capacity of multi-antenna Gaussian channels," *Eur. Trans. Telecommun.*, vol. 10, no. 6, pp. 585–595, 1999.
[42] J. Salo, P. Suvikunnas, H. M. El-Sallabi, and P. Vainikainen, "Ellipticity statistic as measure of MIMO multipath richness," *Electron. Lett.*, vol. 42, no. 3, pp. 160–162, Feb. 2006.
[43] Q. H. Abbasi, H. El Sallabi, E. Serpedin, K. Qaraqe, A. Alomainy, and Y. Hao, "Ellipticity statistics of ultra wideband MIMO channels for body centric wireless communication," in *Proc. 10th Eur. Conf. Antennas Propag. (EuCAP)*, Apr. 2016, pp. 1–4.

**DAZHI PIAO** received the B.S. and M.S. degrees in communication engineering from the Guilin University of Electronic Technology, Guilin, China, in 1999 and 2002, respectively, and the Ph.D. degree in signal and information processing from the Institute of Acoustics, Chinese Academy of Sciences, Beijing, China, in 2006.

Since 2006, she has been with the Department of Communication Engineering, Communication University of China, Beijing, where she has been a Full Professor, since 2014. From 2009 to 2011, she was a Postdoctoral Fellow with the Department of Electronic Engineering, Tsinghua University, Beijing. Her research interests include wireless communications, multiple-input multiple-output antenna design, and channel modeling.

**YAJIN WANG** received the B.S. degree in communication engineering from Henan Normal University, Xinxiang, China, in 2014, and the M.S. degree in communication and information system from the Communication University of China, Beijing, China, in 2018, where she is currently pursuing the Ph.D. degree. Her current research interests include antennas, metamaterials, and radar target characteristics.